Journal of Hydrology 637 (2024) 131343

Contents lists available at ScienceDirect

Journal of Hydrology

journal homepage: www.elsevier.com/locate/jhydrol

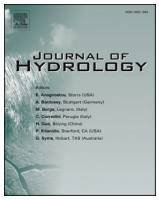

Research papers

Effects of layered heterogeneity on mixed physical barrier performance to prevent seawater intrusion in coastal aquifers

Antoifi Abdoulhalik [a,*], Ashraf A Ahmed [a,*], Ismail Abd-Elaty [b]

[a] Department of Civil and Environmental Engineering, Brunel University London, Kingston Lane Uxbridge UB83PH, United Kingdom
[b] Department of Water and Water Structures Engineering, Faculty of Engineering, Zagazig University, Zagazig 44519, Egypt

ARTICLE INFO

This manuscript was handled by Mohsen M. Sherif, Editor-in-Chief, with the assistance of Corrado Corradini, Associate Editor

Keywords:
Cutoff walls
Subsurface dams
Sea-level rise
Laboratory experiments
SEAWAT
Climate Change Impact

ABSTRACT

Mixed physical barriers (MPB), which combine a cutoff wall and subsurface dam, were applied in heterogeneous coastal aquifer settings, and their ability to prevent seawater intrusion (SWI) was tested. The performance of MPB was examined in a typical stratified aquifer using laboratory experiments and numerical modelling. The performance of the MPB was compared to that of a single cut-off wall by measuring the percentage of reduction of the intrusion length. SEAWAT was used for validation purposes and to further evaluate the effectiveness of MPB in five additional realistic heterogeneous configurations. Experimental results show that the MPB effectively reduced the saltwater wedge length by up to 71%. The MPB outperformed the single cut-off wall by up to 55 %. Also, numerical results show that the MPB proved to be effective, achieving a SWI length reduction of up to 69% in the scenario regardless of the aquifer layering structures. Comparable performance was observed when the high K layer was confined between two low K layers or when the aquifer presented a monotonically increasing/decreasing K pattern. The findings of this study provide insights into the applicability of the MPB in realistic heterogeneous coastal aquifers.

1. Introduction

Seawater intrusion (SWI) in coastal aquifers essentially results from excessive groundwater abstraction and is further exacerbated by climate-change-related factors (drought and sea-level rise). SWI leads to detrimental effects that are difficult to remediate, including the salinisation of coastal groundwater reservoirs and the abandonment of pumping wells (Werner et al., 2013). The expected increase in the global population in coastal areas (Alfarrah and Walraevens, 2018; Yu et al., 2019), as well as the forecasted sea level rise (IPCC, 2013), will ultimately lead to further SWI and thus cause more deterioration of coastal groundwaters worldwide.

Effective mitigation of SWI requires implementing practical measures to control or reduce landward saltwater penetration. Various practical measures have been implemented to protect coastal aquifers from SWI. The most common countermeasures involve reducing groundwater abstraction (Abarca et al., 2006; Ketabchi and Ataie-Ashtiani, 2015), changing the pumping wells locations (Mantoglou and Papantoniou, 2008), injecting freshwater through infiltration basins, canals, recharge ponds, or wells to create positive hydraulic barriers (Luyun et al., 2011, Lu et al., 2017), abstracting saline water from the saltwater wedge to form a negative hydraulic barrier (Pool and Carrera, 2010), constructing subsurface physical barriers (Kaleris and Ziogas, 2013, Abdoulhalik et al., 2017) or a combination of the one or more of the above methods (Abd-Elaty et al., 2021). The injection of subsurface compressed air has also recently been explored and has proven to be quite effective in controlling SWI (Zang and Li, 2021; Zang et al., 2023).

Subsurface barriers are among the most commonly used strategies in practical engineering solutions. They have been successfully implemented in various countries, including Japan, China, India, the Middle East, and some African countries (Janardhana Raju et al., 2013; Stevanović, 2016). Three different types of subsurface barriers have been proposed in previous literature, which include fully penetrating subsurface barriers, subsurface dams, and cutoff walls. Fully penetrating subsurface barriers are semi-permeable and extend from the aquifer bedrock to the top of the aquifer (Kaleris and Ziogas, 2013). Subsurface dams generally exhibit a very low permeability and extend from the aquifer bottom to a specific height that blocks only the lower part of the aquifer cross-section while enabling seaward groundwater discharge in

* Corresponding authors.
E-mail addresses: antoifi.abdoulhalik@brunel.ac.uk (A. Abdoulhalik), ashraf.ahmed@brunel.ac.uk (A.A. Ahmed).

https://doi.org/10.1016/j.jhydrol.2024.131343
Received 3 January 2024; Received in revised form 26 March 2024; Accepted 1 May 2024
Available online 14 May 2024
0022-1694/© 2024 The Author(s). Published by Elsevier B.V. This is an open access article under the CC BY license (http://creativecommons.org/licenses/by/4.0/).

the upper part (Luyun et al., 2009; Abdoulhalik and Ahmed, 2017a). Cut-off walls are also of very low permeability and extend from the top of the aquifer to a specific penetration depth, such that to block the upper part of the aquifer (Anwar, 1983; Kaleris and Ziogas, 2013; Abdoulhalik et al., 2017; Abdoulhalik and Ahmed, 2017b; Abdoulhalik et al., 2020; Abd-Elaty and Zelenakova, 2022).

In addition to these traditional physical barriers mentioned above, Abdoulhalik et al. (2017) proposed a mixed physical barrier (MPB) as a new SWI control method, combining a cutoff wall and a semi-permeable subsurface dam. Due to the specific structure and the associated saltwater lifting mechanism generated, they demonstrated that the MPB could outperform the semi-permeable dam and the single cutoff wall by achieving up to 62 % and 42 % more saltwater intrusion length reduction, respectively. Furthering the work of Abdoulhalik et al. (2017), Gao et al. (2021) used a subsurface dam with low permeability and tested the ability of the MPB system to remove residual saline water and assessed its impact on groundwater discharge dynamics. Their study evidenced the superiority of MPB over traditional subsurface dams and cut-off walls, achieving up to 40 %-100 % and 0 %-56 % more residual saltwater removal, respectively. Lately, Wang et al. (2023) further investigated the performance of MPB in SWI control and explored its impact on nitrate pollution accumulation in coastal aquifers. They showed that the installation of MPB resulted in an exacerbation of nitrate concentration and the area of nitrate contamination within the aquifer. Although they demonstrated that, in terms of SWI control, the MPB was 46–53 % and 16–57 % more effective than traditional subsurface dams and cut-off walls, respectively, the construction of the MPB resulted in more severe nitrate pollution accumulation. Specifically, the MPB induced 14–27 % and 2–12 % more nitrate accumulation than conventional subsurface dams and cut-off walls, respectively. Their findings highlight the importance of careful design selection in constructing MPB to limit the accumulation of nitrate pollutants without compromising its performance in controlling SWI.

Although the MPB system has great potential for protecting coastal groundwater from SWI, all previous MPB-related studies assumed homogenous and isotropic aquifer conditions and did not consider subsurface heterogeneity. Real-life coastal aquifers generally exhibit complex geological heterogeneous structures that disrupt groundwater flow and alter saltwater intrusion dynamics (Simmons et al., 2001). A large number of coastal aquifers present layered patterns (Mehdizadeh et al., 2014; Mehdizadeh et al., 2017; Strack and Ausk, 2015), typically with a low-permeability layer that is confined between two layers of high permeability (Kim et al., 2006; Ratner-Narovlansky et al., 2020).

Previous studies have well established that such layered heterogeneous structures tend to significantly impact the performance of subsurface barriers in controlling SWI (e.g., Abdoulhalik and Ahmed, 2017a; Abdoulhalik and Ahmed, 2017b). Abdoulhalik and Ahmed (2017a) showed that cut-off walls could remain effective regardless of the layered patterns, albeit their performance was enhanced in systems bearing a low permeability layer in the upper part of the aquifer. Likewise, the performance of subsurface dams in removing residual saline water was improved when a low K layer was at the top of the aquifer and worsened when it was at the bottom, whereby total removal of residual saltwater took nearly 50 % longer than in the homogeneous case (Abdoulhalik and Ahmed, 2017b). These aforementioned studies that assessed the performance of subsurface barriers while incorporating ground heterogeneity were conducted for conventional barriers (cut-off and subsurface dam). To the best of our knowledge, no study has attempted to examine the effectiveness of MPB in controlling SWI under heterogeneous conditions using physical experiments, which are well-known for conveniently providing a more realistic representation of the hydrodynamics and transport processes occurring in real-world conditions.

This study aims to provide insight into the ability of MPB to prevent SWI in typical layered coastal aquifers. The performance of MPB was examined in a typical layered heterogeneous coastal aquifer using laboratory and numerical experiments. The freshwater head boundary was varied to impose different hydraulic gradient conditions, and subsequently, various saltwater intrusion scenarios and salt concentration maps were derived using automated image analysis techniques. The SEAWAT code was used for validation purposes and to test the MPB further in five realistic heterogeneous scenarios. The performance of the MPB was measured in terms of the percentage of reduction of the saltwater intrusion length and salt content in the aquifer.

2. Material and methods

2.1. Experimental methods

Laboratory experiments were conducted in a head-controlled flow tank composed of a main central chamber flanked by side reservoirs, as shown in Fig. 1. The central chamber, which was 0.38 m × 0.15 m x 0.01 m, was filled with clear glass beads to reproduce the porous medium. The glass beads were siphoned into the chamber under fully saturated conditions to prevent air from being trapped in the system.

The simulation of heterogeneity effects, as well as the semi-permeability of the subsurface dam, required the use of beads of different mean diameters, namely 1090 μm, 425 μm, and 300 μm. The hydraulic conductivity K values of the beads were previously derived through volumetric freshwater discharge measurement within the flow tank (Oostrom et al., (1992). The hydraulic conductivity of the beads 1090 μm, 425 μm, and 300 μm were estimated at 85 cm/min, 17 cm/min, and 10 cm/min, respectively.

The freshwater head boundary was set on the left-side reservoir, while the saltwater head boundary condition was set on the right-side reservoir. The saltwater solution was prepared by dissolving commercial salt into freshwater at a concentration of 36.16 g/L to achieve a 1025 kg/m^3 density (Robinson et al., 2015). A hydrometer H-B Durac plain-form polycarbonate was used to monitor saltwater density. For clearer visualisation of the SWI process, a red food colour was used to dye the saltwater solution. In each reservoir, an overflow outlet was used to drain any excess water to waste and thus conveniently adjust the water level. Ultrasonic sensors were used to monitor the water levels precisely throughout the experiments.

Two LED lights (Camtree 600) were placed behind the experimental set-up to illuminate the porous media. Images of the experiments were recorded using a camera IDT MotionPro X-Series.

2.2. Experimental procedure

The effectiveness of the MPB was examined in a heterogeneous configuration with a three-layer aquifer of configuration high K – low K – high K, as typically found in real-world coastal aquifers (Fig. 2). The beads of size 1090 μm were used to simulate the high K layers (top and bottom), while the beads 425 μm were used to reproduce the middle layer of low K. The assessment of the performance of the MPB in the layered configuration required first the analysis of SWI in a similar heterogeneous setting with no barrier (base case) for reference purpose. In addition, another configuration was analysed where the subsurface dam was removed to compare the performance of the MPB to that of a traditional cutoff wall in a heterogeneous setting. Performance was characterised by the ability of the barrier to restrict the intruding saltwater, which was defined as the percentage reduction of the intrusion length R, with $R = (X_0 - X_B)/X_0$, where X_0 is the intrusion length before the installation of the barrier, and X_B is the intrusion length after the barrier has been installed.

The cut-off wall was simulated using impermeable material (plasticine) within the saltwater wedge area for optimal performance (Luyun et al., 2011). The cut-off wall was placed at 6.60 cm from the saltwater side with a width of 2 cm, and the opening to the aquifer bottom was 1.60 cm such that the depth of the cutoff wall exceeded 60 % of the aquifer thickness (Kaleris and Ziogas, 2013). The semi-permeable dam

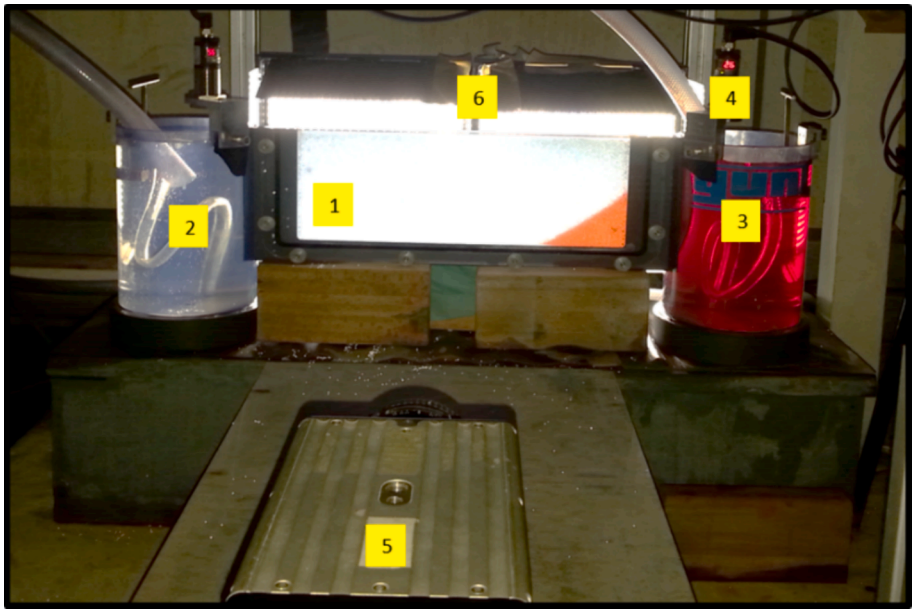

Fig. 1. Laboratory set-up; 1) Central chamber; 2) Freshwater side; 3) Saltwater side; 4) Sensors; 5) Camera; 6) Background lights.

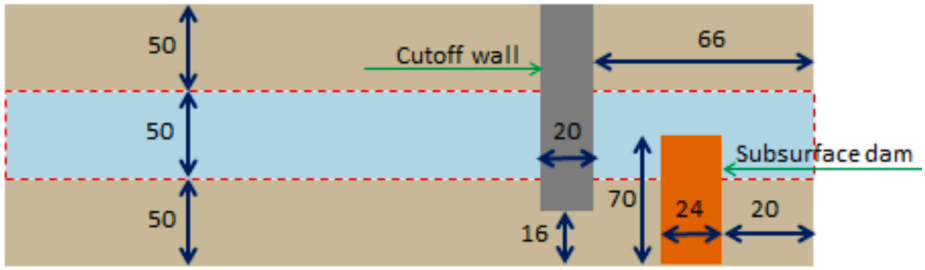

Fig. 2. Schematic design of the MPB configuration. The dimensions are in mm.

was simulated using fine beads of size 300 μm, which were siphoned into the system to a height of 7 cm. and a thickness of 2.4 cm before the packing of the coarse beads (Table 1).

Changes in the hydrological conditions were simulated imposing various hydraulic gradients to the system. While the freshwater head boundary was varied, the seaside boundary remained constant. Upon initiating the experiment, the saltwater level was set to 12.97 cm while the freshwater level was set sufficiently high to prevent any intrusion of saline water and thus maintain the porous media fully saturated with freshwater. Note that the hydraulic gradient values tested herein have commonly been used in previous laboratory studies (Goswami and Clement, 2007; Chang and Clement, 2012; Abdoulhalik et al., 2017; Abdoulhalik et al., 2022) and are also comparable with values observed in real aquifer systems (Ferguson and Gleeson, 2012; Attanayake and Sholley, 2007).

Before each experimental test, a calibration procedure was performed to determine the main SWI intrusion parameters accurately and produce salt concentration maps. The toe length of the saltwater wedge was taken as the distance between the 50 % concentration isoline and the saltwater boundary along the bottom boundary.

2.3. Numerical model and procedure

The SEAWAT code (Guo and Langevin, 2002) was used here for the numerical modelling experiments. SEAWAT has been widely used to solve various variable-density groundwater flow problems (Guo and Langevin, 2002; Langevin et al., 2003) and for modelling SWI experiments (Abdoulhalik and Ahmed, 2017a; Goswami and Clement, 2007; Chang and Clement, 2012). SEAWAT simulations were performed for validation purposes and to develop additional models to assess better the performance of the MPB in various heterogeneous aquifer systems.

The variable-density groundwater flow equation (Guo and Langevin, 2002) solved by the Variable-Density Flow (VDF) Process is as follows:

$$\nabla\left[\rho^{*}\frac{\mu_o}{\mu}{*}K_o\left(\nabla^{*}h_0+\frac{\rho-\rho_f}{\rho_f}{*}\nabla Z\right)\right]=\rho^{*}S_{s,0}\left(\frac{\partial h_O}{\partial t}\right)+\theta^{*}\left(\frac{\partial \rho}{\partial C}\right)\left(\frac{\partial C}{\partial t}\right)-\rho_s{*}q_s^{\backslash} \quad (1)$$

The solute transport equation (Zheng et al., 1999) solved by the Integrated MT3DMS Transport (IMT) process is as follows:

$$\left(1+\frac{\rho_b{*}K_d^k}{\theta}\right)\frac{\partial(\theta^{*}C)}{\partial t}=\nabla\left(\theta D^{*}\nabla C^k\right)-\nabla\left(q^{*}C^k\right)-\left(q_s^{\backslash}{*}C_s^k\right) \quad (2)$$

Table 1
Hydraulic parameters and boundary condition of the experimental procedure.

Geometry	Value	Dimension
X; Z; Y	38, 15, 1	cm
Aquifer Hydraulic Parameters	**Value**	**Dimension**
Freshwater density (ρf)	1000	$kg.m^{-3}$
Saltwater density (ρs)	1025	$kg.m^{-3}$
Specific Storage	10^{-6}	cm^{-1}
Longitudinal dispersivity (αL)	1	cm
Transverse dispersivity (αT)	0.50	cm
Molecular diffusion coefficient(D*)	0	m^2 day^{-1}
Beads mean diameters for top and bottom layers (high K)	1090	μm
Beads mean diameters for middle layer (low K)	425	μm
Hydraulic conductivity (k) (Isotropic) for top and bottom layers	85	cm min^{-1}
Hydraulic conductivity (k) (Isotropic) for middle layer	17	cm min^{-1}
Aquifer Boundary Condition	**Value**	**Dimension**
Saltwater head	12.97	cm
Initial freshwater head	13.57	cm
Final freshwater head	13.37	cm
Seaside concentration (Cs)	36.16	g L^{-1}
Landside concentration (C_0)	0	g L^{-1}
Cutoff wall	**Value**	**Dimension**
Distance from the seaside	6.60	cm
Opening depth	1.60	cm
Beads mean diameters	300	μm
Hydraulic conductivity (k)	$1x10^{-5}$	cm min^{-1}
Subsurface dam	**Value**	**Dimension**
Distance from the seaside	20	cm
Dam height	7	cm
Beads mean diameters	300	μm
Hydraulic conductivity (k)	10	cm min^{-1}

where C: is the salt concentration [ML^{-3}]; q'$_s$: is a source or sink [T^{-1}] of fluid with density ρ_s, ρ_b: is the bulk density [ML^{-3}], ρ_o: is the fluid density [ML^{-3}], ρ: is the saltwater density [ML^{-3}], μ_o: is the dynamic freshwater viscosity [$ML^{-1}T^{-1}$], μ: is the saltwater dynamic viscosity [ML^{-1} T^{-1}], K_0: is the hydraulic conductivity [LT^{-1}], h_0: is the hydraulic head [L], q: is the specific discharge [LT^{-1}], D: is the hydrodynamic dispersion coefficient [L^2T^{-1}], $S_{s,0}$: is the specific storage [L^{-1}], t: is the time [T]; θ: is the porosity [-]; K_d^k: is the distribution coefficient of species k [L^3/M], C_k: is the concentration of species k [ML^{-3}], and C_s^k: is the source or sink concentration [ML^{-3}] of species k.

The dimensions of the simulation area were the same as the laboratory central chamber. The grid size was set to 0.2 cm. The longitudinal dispersivity was 0.1 cm, while the transverse dispersivity was set to 0.05 cm. These values are within the range of values used in similar studies (e.g., Abarca and Clement, 2009). Peclet number was inferior to four, which satisfied numerical stability (Voss and Souza, 1987). The specific storage was set to 10^{-6} cm^{-1}, and the molecular diffusion was neglected (Riva et al., 2015). The freshwater and saltwater density values were set to 1000 kg/m^3 and 1025 kg/m^3, respectively. The semi-permeability of the subsurface dam was reproduced by setting a very low hydraulic conductivity to the cells of interest (10 cm/min). The cut-off wall was modelled by considering the cells of interest as inactivated.

At the start of the simulation, the freshwater head was set to 13.57 cm and the saltwater head to 12.97 cm, which allowed saline water to enter the system. As in the experiments, the freshwater head boundary was then changed to impose a head difference dh = 4 mm (advancing phase) and dh = 6 mm (receding phase). The model was allowed to run for sufficient time for each head change to reach steady state conditions.

3. Results and discussion

3.1. Experimental results

Fig. 3 presents the concentration colour map of the base cases (no barrier) of the two head differences. The initial condition started by setting a freshwater boundary head of 13.57 cm, which imposed a head

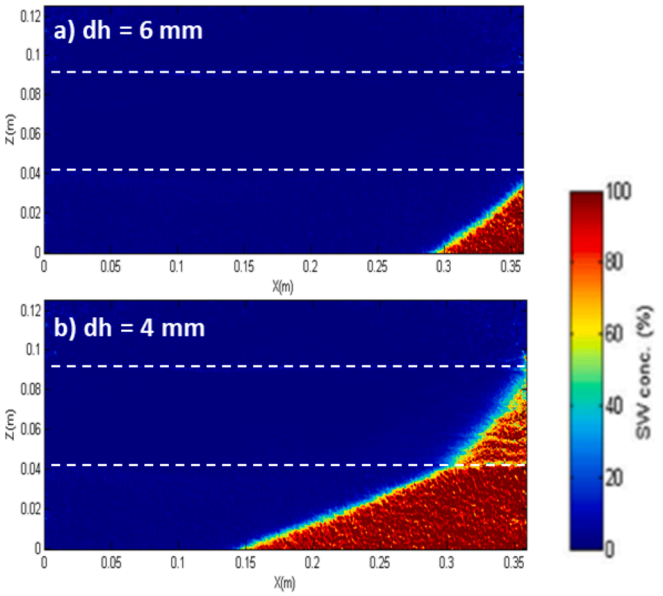

Fig. 3. Steady-state experimental toe length in the base case for the two hydraulic gradients applied. The dashed lines represent the upper and lower interlayer boundaries.

difference of dh = 6 mm on the system. This head change disrupted the system's equilibrium and allowed the saline water to penetrate the porous medium until the system reached the first steady state condition. The steady-state toe length was also relatively short, and the thickness of the saltwater wedge along the seaside boundary was limited by the edge of the low K layer.

The freshwater head was further decreased to impose a head difference dh = 4 mm. The freshwater head drop caused further saltwater intrusion into the porous medium, forming a slightly distorted saltwater wedge compared to the idealised wedge-like observed in a homogeneous setting, which was also associated with a transition zone widening within the low K layer. Similar observations were reported in previous similar aquifer settings (Abdoulhalik and Ahmed, 2017a).

Fig. 4 presents the concentration colour map of the MPB cases for the

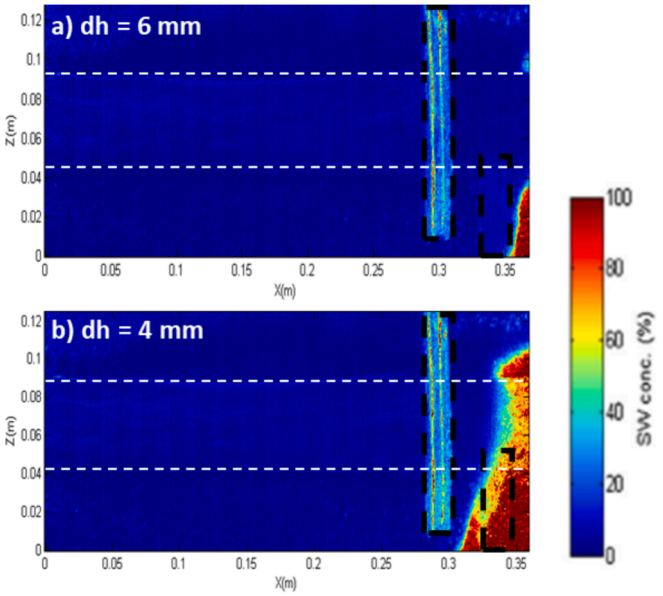

Fig. 4. Steady-state experimental toe length in the MPB case for the two hydraulic gradients applied; a) The dashed lines represent the upper and lower interlayer boundaries.

two head differences tested. After imposing the initial boundary condition to the system (dh = 6 mm), the saline water entered the system only in the high permeability parts of the aquifer. The saline water did not penetrate the low K layer, significantly reducing the intrusion length. The landward incursion of the saline water prompted by the freshwater drop (dh = 4 mm) did not penetrate beyond the cut-off wall position. The saltwater penetrated more into the top high K zone. Again, the freshwater-saltwater transition zone widening occurred, but the widening was substantially greater and extended from the upper part of the bottom high K layer within the location of the subsurface dam and throughout the entire thickness of the middle-low K layer.

In the base case, the low K interlayer drove freshwater to flow in the higher permeability zones, i.e., on the top and bottom parts of the aquifer. The freshwater flowing in the top high K layer does not contribute to repulsing the saltwater but directly exits the system. On the contrary, the freshwater flow in the lower high K layer greatly pushes the wedge toward the seaside boundary, resulting in a shorter wedge than the homogeneous scenario. Such distortion of the wedge was observed in previous similar configurations in Abdoulhalik and Ahmed (2017 a, b).

After the installation of the MPB, the intrusion rate was nonetheless noticeably delayed by the presence of the semi-permeable dam. The increase of the flow velocity through the wall opening, therefore, increased the velocity ratio between the seaward freshwater flow and the density-driven intruding wedge, thereby causing the upward lifting of saline water above the dam, as reported in Abdoulhalik et al. (2017). Fig. 4b shows significant spreading of the freshwater-saltwater transition zone within the location of the subsurface dam and in the middle layer of low K.

The temporal evolution of the saltwater intrusion length in the MPB case was compared to that of the base case (Fig. 5). In addition, the transient toe length of a scenario without a semi-permeable dam was also shown to effectively compare the effectiveness of the MPB system to that of a traditional cut-off wall in a similar heterogeneous configuration. The design parameters of the impermeable wall were the same as those used in the MPB case. In all cases, the minor fluctuations observed in the toe length were probably due to occasional water level changes within the side reservoirs resulting from surrounding vibrations occurring throughout the experiments.

Following the first freshwater head drop (dh = 6 mm), the saltwater wedge length extended up 7 cm in the base case, and the steady state was reached within the first 15 min. In the MPB case, saline water intrusion length only extended up to 2 cm, while it extended up to 4.4 cm in the scenario without the semi-permeable dam (cut-off wall only). In both cases, steady-state was reached within 5 min after the start of the experiment.

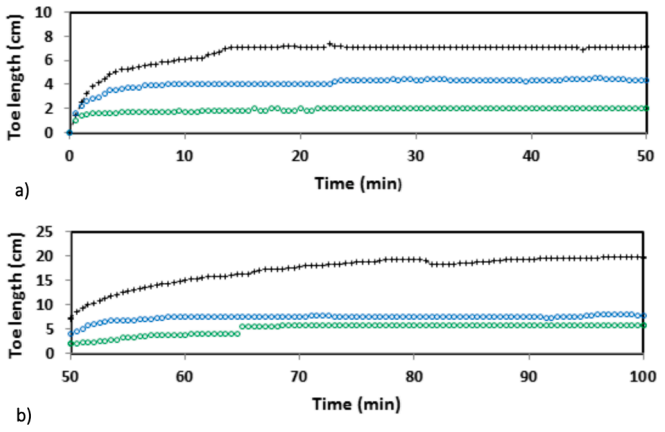

Fig. 5. Experimental transient toe length data in the base case (black), in the MPB case (green) and the cutoff wall case (blue); (top) dh = 6 mm and (bottom) dh = 4 mm. (For interpretation of the references to colour in this figure legend, the reader is referred to the web version of this article.)

Following the decrement of the freshwater head (dh = 4 mm), the saltwater wedge length reached about 19.7 cm at steady state, while it only reached 5.7 cm in the MPB case. Hence, the MPB system effectively reduced the saltwater intrusion length by about 71 % in the two head differences scenarios. In the cut-off wall case, the steady-state toe length extended up to 7.8 cm. Therefore, adding the semi-permeable dam associated with the MPB system resulted in an additional intrusion length reduction of 55 % and 27 %, for dh = 6 mm, and dh = 4 mm. While Abdoulhalik et al. (2017) demonstrated the performance of the MPB as a new SWI control method; these results suggest that this barrier system could effectively reduce saltwater wedge length in such a typical heterogeneous coastal aquifer setting.

3.2. Numerical modelling

Numerical validation was done through qualitative comparison between the saltwater wedge shape in the experimental and numerical simulations at steady-state (Fig. 6). For both head differences tested, the numerical model reproduced the shape of the saltwater wedge very well, in terms of freshwater-saltwater transition-zone dynamics (narrowing and widening) and the extent of the saltwater intrusion length.

3.2.1. Impact of hydraulic gradients on SWI

The numerical model could reproduce the response of the freshwater-saltwater transition zone to the variations of hydraulic gradients. In the base case, the model reproduced the evolution of the transition zone shape from narrow to wide, as observed at dh = 6 mm and dh = 4 mm, respectively. At dh = 6 mm, the saltwater wedge remained within the high permeability zone and did not cross the low K layer, exhibiting a thin transition zone. At dh = 4 mm, the shape of the freshwater-saltwater transition zone substantially widens as it intersects the low K middle layer, as observed in the experiments, although the transition zone exhibited in the numerical model was slightly wider than the experimental model. In the MPB case, the widening of the transition zone occurring within the semi-permeable dam as well as the low K layer was also well replicated at dh = 4 mm. Some discrepancies were observed within the low K layer at dh = 6 mm, whereby no intrusion occurred in the middle layer in the experimental, while small part of the wedge was visible in the numerical model, albeit with low concentration part of the transition zone.

The extent of the saltwater wedge produced in the numerical simulations was relatively close to the values previously measured in the physical model. In the base case, the wedge was relatively small, with an intrusion length of about 8.7 cm at for dh = 6 mm. The total salt content per unit volume of the aquifer was estimated at 0.41 kg. At dh = 4 mm, the shape of the saltwater wedge matched the experimental observations, with a visible distortion as the transition zone crossed the interlayer boundary. The toe length was about 22.8 cm at steady-state, which is relatively close to the value measured in the physical experiment. The estimated salt content per unit volume of the aquifer increased to 1.72 kg—the results in terms of intrusion length and aquifer salt volume. The salt content variation (C-C0)/C0 were calculated to monitor the salinity within the aquifer, where C0 and C refer to the initial salt concentration and the salt concentration in a given case, respectively (Abd-Elatyet al., 2019). A positive value indicated that the salt content has increased compared to the base case, while a negative value implies that salt was removed from the aquifer, i.e., the MPB induced a positive effect on SWI.

3.2.2. Impact of aquifer heterogeneous on SWI using MPB

To further examine the effectiveness of the MPB in heterogeneous conditions, three additional scenarios where the low K layer was placed at different elevations (Fig. 8). The first scenario had a low K layer at the top part of the system, i.e., Low K- High K (case LH), the second scenario had a low K layer at the bottom part of the system, i.e., High K- Low K (case HL), and the last scenario had a low K layer at the top and bottom

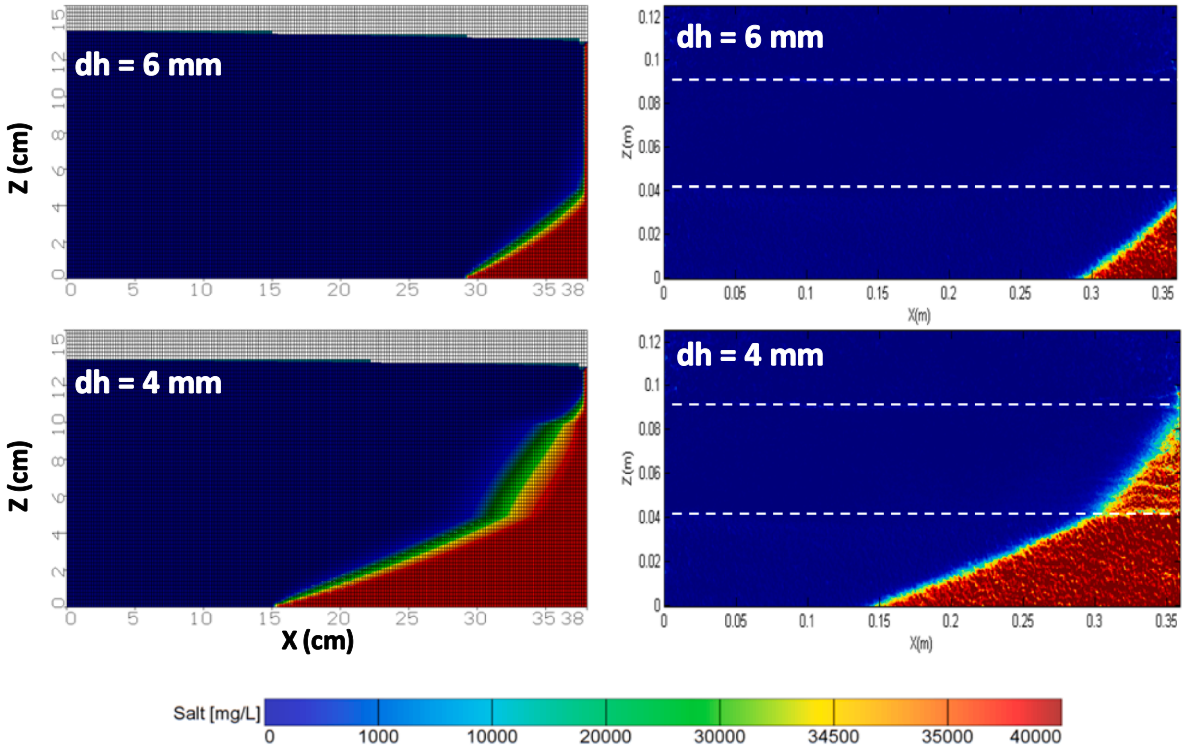

Fig. 6. Comparison between numerical (left) and experimental (right) saltwater wedge in case of HLH before MPB installation, for dh = 6 mm (top) and dh = 4 mm (bottom).

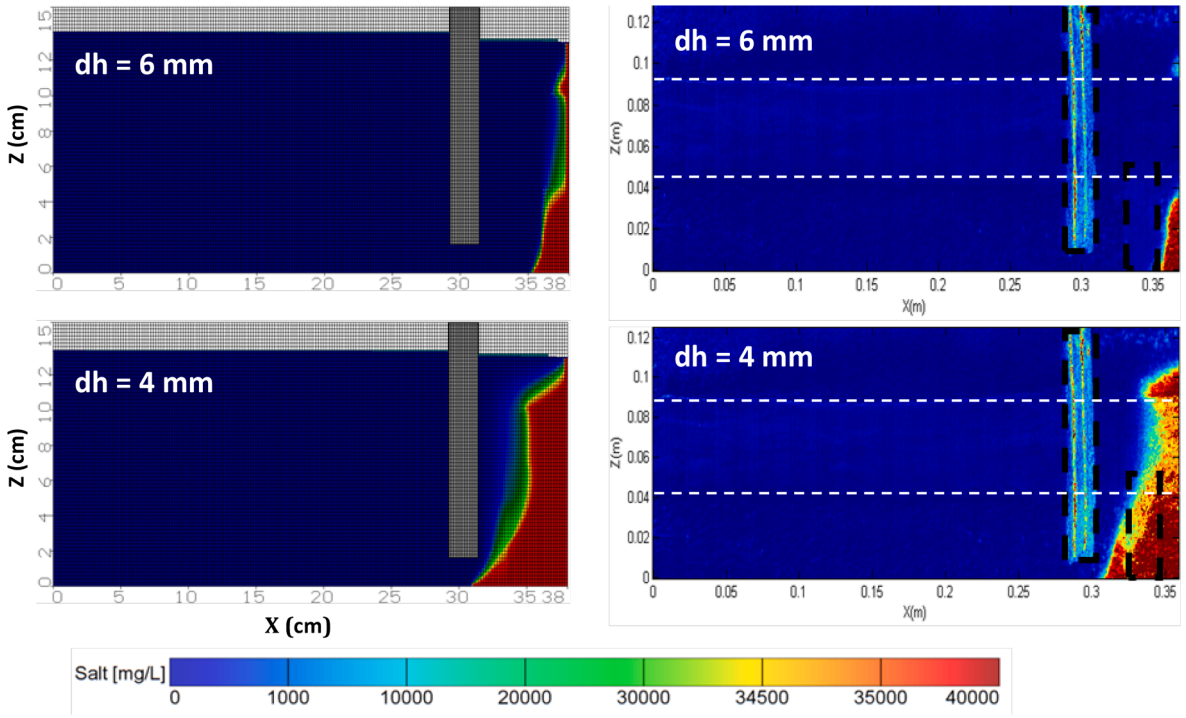

Fig. 7. Comparison between numerical (left) and experimental (right) saltwater wedge in case HLH after MPB installation, for head difference dh = 6 mm (top) and dh = 4 mm (bottom).

of the aquifer, i.e., Low K-High K- Low K (case LHL).

The numerical model also replicated the shape of the saltwater wedge in the MPB case (Fig. 7). At dh = 6 mm, most of the intrusion occurred in the lower portion of the aquifer in the high K permeability zone, where the subsurface dam restricted it. The recorded toe length was 2.7 cm at a steady state. No substantial intrusion was observed in the middle low K layer, and very little saline water intruded into the top high K layer. The salt content per unit volume in the aquifer was only 0.20 kg at steady state. At dh = 4 mm, the intrusion length was about 7 cm, comparable to the value measured in the physical experiments. The

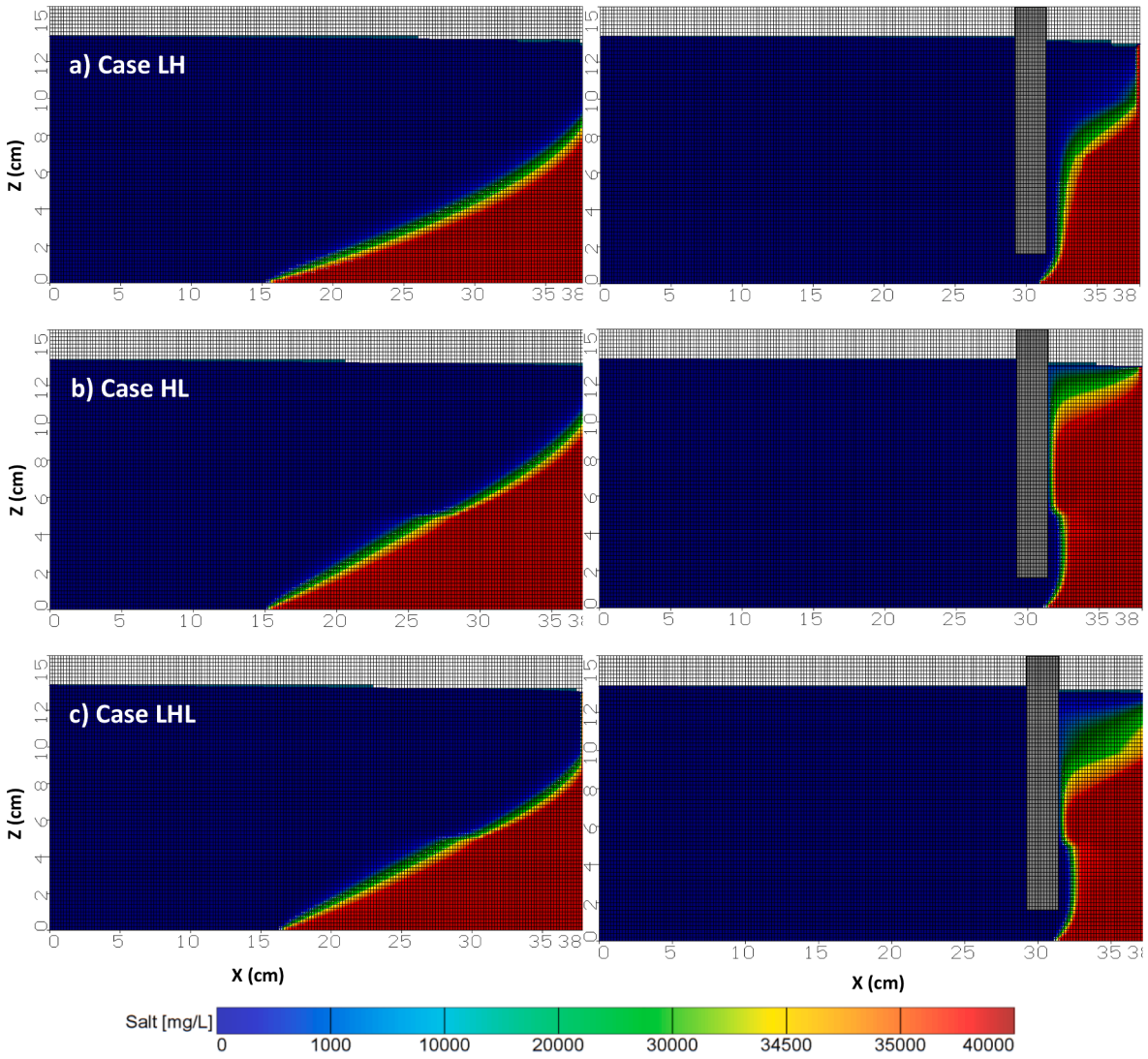

Fig. 8. Numerical saltwater wedge in a) case LH, b) case HL, and c) case LHL before (left) and after (right) the installation of the MPB for a head difference dh = 4 mm.

aquifer's salt content per unit volume was 0.77 kg at steady-state. In other words, at dh = 6 mm, installing the MPB system reduced the saltwater intrusion length by 69 % and removed nearly 44 % of the total salt content initially present in the aquifer system. At dh = 4 mm, the MPB reduced the saltwater intrusion length by 69 % and the total salt content in the aquifer by 75 %. Hence, the numerical simulations further demonstrated the performance of the MPB system in repulsing saltwater intrusion in typical layered heterogeneous conditions.

In case LH, the intrusion length recorded at a steady state was 22.6 cm and 7.1 cm before and after MPB installation, respectively. This corresponds to a reduction of the saltwater intrusion length of 69 %. Before the installation of the MPB, the amount of salt per unit volume of the aquifer was about 1.59 kg. This amount was reduced by 50 % after installing the MPB system, leaving only 0.80 kg in the aquifer. Case HL exhibited an intrusion length of 22.9 cm before MPB installation and decreased to 6.7 cm thereafter, thereby achieving 70 % toe length reduction (Fig. 8b). The amount of salt in the aquifer decreased from 2.07 kg to 1.13 kg (i.e., 45 %) after the MPB installation. In the case of LHL, the toe length extended to 21.4 cm before wall installation and was reduced to 6.9 cm after installing the MPB, i.e., a reduction of 68 % (Fig. 8c). Also, the MPB reduced the salt content of the unit volume of the aquifer from 1.75 kg to 0.99 kg, thereby decreasing the amount of salt by 43 %. These results show that the MPB could achieve substantial saltwater repulsion regardless of the elevation of the low K layer in the aquifer system.

The results show that the retreat of the saltwater wedge presented a distorted shape and transition zone to various degrees depending on the stratification pattern. The wedge thickness along the seaside boundary was visibly shorter in case LH, while it nearly approached the upper limit of the aquifer in case HL. The thickness observed in case LHL was comparable to that of case LH, but the transition zone was noticeably wider in the latter than in the former, and the widening was also more spread over the length of the transition zone. Such an elongated transition zone was also observed in scenario HLH (Fig. 7), but the thickness along the seaside boundary was shorted in scenario LH. The saltwater wedge behaviour suggests that the intensity of seaward freshwater flow was greater in cases LH than in the other scenarios.

In scenario LH, the upper layer of low K forces downward freshwater flow in the lower part of the aquifer, which is then further enhanced below the wall with increased velocity, thereby causing both the seaward shifting of the toe and a reduction of the overall salt content within the aquifer. The increased freshwater flow is also responsible for more pronounced widening and the reduced wedge thickness along the seaside boundary, where freshwater exits towards the outlet. A similar process occurred in scenario HLH, but to a lesser extent as the low K layer in the middle portion of the aquifer partly restricted the downward

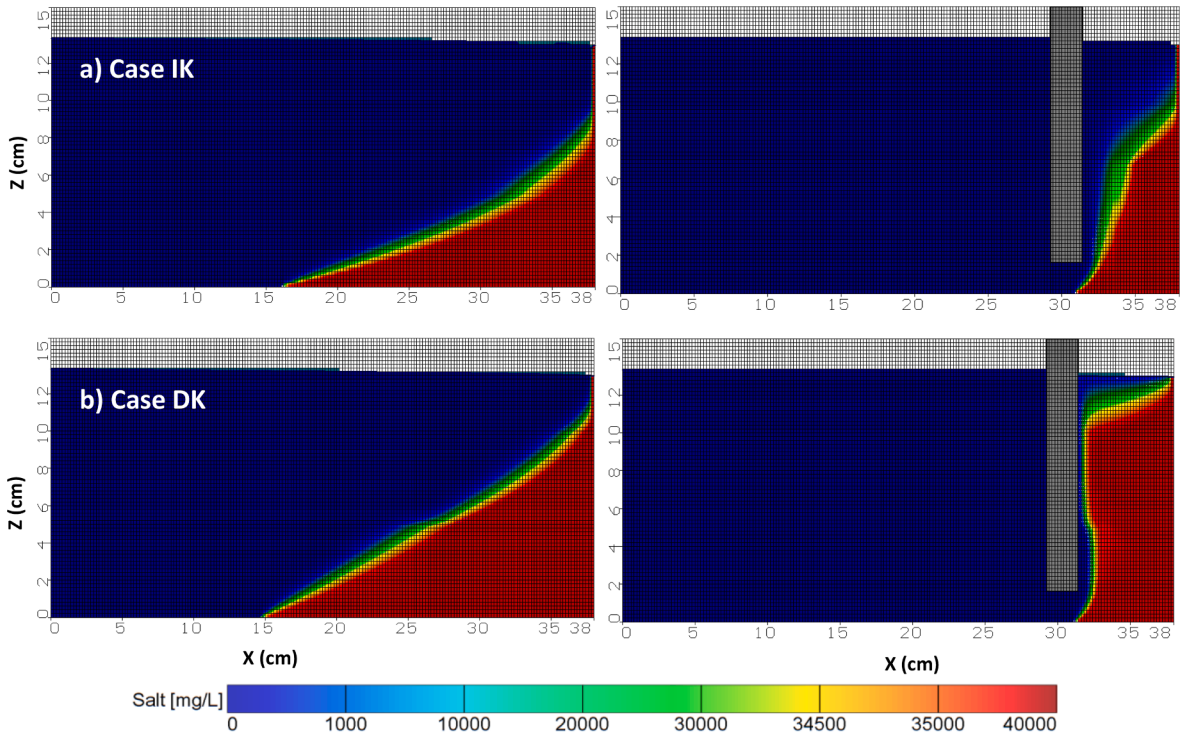

Fig. 9. Numerical saltwater wedge in additional heterogeneous scenarios with a) increasing K (case IK), and b) decreasing K (case DK) from top to bottom of the aquifer, before (left) and after (right) the installation of the MPB for a head difference dh = 4 mm.

movement of the freshwater flow towards the wall opening. In case HL, the low K layer tend to restrict the freshwater flow transiting in the lower layer where it is needed to effectively repulse the saline water, thereby limiting the effectiveness of the MPB.

3.2.3. *Impact of aquifer hydraulic conductivity on SWI*

Two additional layered scenarios were investigated whereby the hydraulic conductivity was monotonically increased (case IK) and decreased (case DK) from the top to the bottom of the aquifer (Fig. 9). Specifically, the aquifer in case IK was composed of three layers with a hydraulic conductivity of 17–51-85 cm/min, while the aquifer in case DK had a hydraulic conductivity of 85–51-17 cm/min. The highest and lowest hydraulic conductivity values used here corresponded to those in the base case, i.e., 85 cm/min and 17 cm/min, and that of the middle was set to 51 cm/min, which was the average value.

In case IK, the extent of the toe length was about 21.70 cm and the salt content in the unit volume (1 m^3) of the aquifer was 1.46 kg before the installation of the MPB. After installing the MPB, the toe length was 7 cm, and the salt mass was 0.73 kg, which implies a reduction of the intrusion length and salt mass by 68 % and 50 %, respectively. In case DK, the saltwater wedge length extended up to 23.2 cm inland and the amount of salt for the unit volume of the aquifer reached around 2.17 kg. After installing the MPB, the toe length was reduced to 6.7 cm, and the salt mass for the unit volume of the aquifer was decreased to 1.13 kg. In other words, installing the MPB reduced the intrusion length by 71 % and the amount of salt by 48 %, respectively.

As expected, the response of the saltwater wedge differed depending on the arrangement of the layers. Low K layers at higher elevations induced greater freshwater flow in lower parts of the system, thus slightly shorter saltwater wedge toe length and thickness along the seaside, as well as a homogeneous widening of the transition zone spread over its length essentially driven by dispersion (Fig. 9a), as previously observed in case LH (Fig. 8a). Low K layers located at lower elevations in the aquifer tend to drive the freshwater flow mainly upwards, thereby causing a slight landward shift of toe, and a rather local transition-zone widening mainly controlled by diffusion was observed, as well as a greater saltwater wedge thickness along the seaside, especially after the MPB installation, where its build-up nearly filled the seaward side of the barrier (Fig. 9b).

The disparity of the heterogeneous structures tested enabled us to explore further the impact of layered patterns on the MPB performance and saltwater dynamics. Overall, the MPB system could remain fairly effective in reducing SWI in all the multi-layered systems investigated herein. Similar findings were recently reported by Emara et al. (2024), who showed that MPB could reduce up to 65 % of saltwater intrusion length in typical heterogeneous settings using numerical modelling. The results agree with those of Abdoulhalik and Ahmed (2017a), who investigated the influence of aquifer stratification on the effectiveness of cut-off walls in controlling SWI. Their study showed that their performance was enhanced in systems bearing a low K layer in the upper part of the system. Abdoulhalik and Ahmed (2017b) also found that a low K layer at the top of the aquifer induced a positive contribution to the performance of subsurface dams, while a low-K layer at the bottom had a counter effect.

These results show that assessing the performance of MPBs in homogeneous conditions may ultimately lead to underestimating their performance. Hence, rigorous geological investigations should be undertaken to accurately delineate the underground structures of the aquifer before evaluating the potential ability of MPB to act as an effective SWI control method. Although real-world stratified coastal aquifers often bear more complex layering structures, with non-linear boundaries between layers and higher permeability contrast, the findings of this study provide a first insight into the impact of typical layered patterns on MPBs effectiveness in preventing SWI. The current results are useful for decision-makers and professional engineers in choosing effective techniques for controlling SWI in heterogeneous coastal aquifers.

4. Summary and conclusions

The impact of layered heterogeneity on the ability of mixed physical barriers to control seawater intrusion was examined using laboratory

and numerical experiments. The heterogeneous configuration consisted of a three-layered system where the top and bottom layers had a high permeability, and the interlayer had a low permeability. The SEAWAT code was used to validate the experimental results and to explore further the performance of the MPB five additional layered configurations, whereby in one case, a top low K layer (case LH); in the second case, the bottom low k layer (case HL); a case with a top and bottom low K layers (case LHL); and two additional layered scenarios were investigated whereby the hydraulic conductivity was monotonically increased (case IK) and decreased (case DK) from the top to the bottom of the aquifer. The performance of the MPB was measured in terms of the percentage of reduction of the intrusion length and salt content within the aquifer. The main findings of the study are:

- Experimental results showed that the MPB effectively reduced saltwater length in the heterogeneous setting, achieving up to 71 % for the two hydraulic gradients tested. The numerical model further confirmed the MPB's performance, with a 69 % reduction of the toe length and a 54 % reduction of the total salt content.
- In the heterogeneous configuration tested, the MPB outperformed the traditional cut-off wall, achieving 55 % and 27 % more intrusion length reduction than the latter for head differences dh = 6 mm and dh = 4 mm, respectively.
- Regardless of the heterogeneous structures simulated, the MPB proved to be effective, achieving a saltwater intrusion length reduction of 69 % and 70 % in the scenario where the low K layer was placed at the top and bottom of the aquifer. Comparable performance was observed when the high K layer was confined between two low K layers or when the aquifer presented a monotonically increasing/decreasing K pattern, whereby toe length and salt content reduction values exceeded 60 % and 40 %, respectively, in all tested cases.

The disparity of the heterogeneous structures tested enabled us to explore further the impact of layered patterns on the MPB performance and saltwater dynamics. The presence of the low permeability layer impacted the overall saltwater dynamics (transition zone and thickness) on the seaward side of the MPB to various degrees, depending on its elevation within the aquifer. Overall, the MPB system could effectively reduce SWI in all the multi-layered systems investigated herein.

Although real-world stratified coastal aquifers often bear more complex layering structures, presenting non-linear boundaries between layers and higher permeability contrast, our study provides a first insight into the effect of typical layered patterns on the performance of MPB in controlling and preventing SWI and highlights the importance of considering ground heterogeneity before designing of MPB systems for more realistic evaluation of its performance as SWI countermeasure. Future work should incorporate groundwater abstraction to explore the ability of MPB to prevent pumping well salinisation. Also, additional investigations involving climate-change-induced sea level rise would be of great interest. These investigations will be the topics of forthcoming publications.

CRediT authorship contribution statement

Antoifi Abdoulhalik: Writing – original draft, Formal analysis, Conceptualization. **Ashraf A Ahmed:** Conceptualization, Methodology, Supervision, Writing – review & editing. **Ismail Abd-Elaty:** Software, Validation.

Declaration of competing interest

The authors declare that they have no known competing financial interests or personal relationships that could have appeared to influence the work reported in this paper.

Data availability

No data was used for the research described in the article.

Acknowledgement

The authors wish to thank Queen's University Belfast for providing the facilities for the second author to conduct the experiments while he was associated with them.

References

Abarca, E., Clement, T.P., 2009. A novel approach for characterizing the mixing zone of a saltwater wedge. Geophys. Res. Lett. 36, L06402.
Abarca, E., Vázquez-Suñé, E., Carrera, J., Capino, B., Gámez, D., Batlle, F., 2006. Optimal design of measures to correct seawater intrusion. Water Resour. Res. 42, W09415.
Abd-Elaty, I., Sallam, G.A., Strafacec, S., Scozzari, A., 2019. Effects of climate change on the design of subsurface drainage systems in coastal aquifers in arid/semi-arid regions: Case study of the Nile delta. Sci. Total Environ. J. 672, 283–295. https://doi.org/10.1016/j.scitotenv.2019.03.483.
Abd-Elaty, I., Zelenakova, M., 2022. Saltwater intrusion management in shallow and deep coastal aquifers for high aridity regions. J. Hydrol.: Reg. Stud. 40, 101026.
Abd-Elaty, I., Straface, S., Kuriqi, A., 2021. Sustainable saltwater intrusion management in coastal aquifers under climatic changes for humid and hyper-arid regions. Ecol. Eng. 171, 106382.
Abdoulhalik, A., Ahmed, A., Hamill, G.A., 2017. A new physical barrier system for seawater intrusion control. J. Hydrol. 549, 416–427.
Abdoulhalik, A., Ahmed, A., 2017a. The effectiveness of cutoff walls to control saltwater intrusion in multi-layered coastal aquifers: experimental and numerical study. J. Environ. Manag. 199, 62–73.
Abdoulhalik, A., Ahmed, A., 2017b. How does layered heterogeneity affect the ability of subsurface dams to clean up coastal aquifers contaminated with seawater intrusion? J. Hydrol. 553, 708–721. https://doi.org/10.1016/j.jhydrol.2017.08.044.
Abdoulhalik, A., Abdelgawad, A.M., Ahmed, A., Moutari, S., Hamill, G., 2022. Assessing the protective effect of cutoff walls on groundwater pumping against saltwater upcoming in coastal aquifers. J. Environ. Manag 323, 116200. https://doi.org/10.1016/j.jenvman.2022.116200.
Alfarrah, N., Walraevens, K., 2018. Groundwater overexploitation and seawater intrusion in coastal areas of arid and semi-arid regions. Water 10, 143. https://doi.org/10.3390/w10020143.
Anwar, H., 1983. The effect of a subsurface barrier on the conservation of freshwater in coastal aquifers. Water Res. 17, 1257–1265.
Attanayake, P., Sholley, M., 2007. Evaluation of the hydraulic gradient at an island for low-level nuclear waste disposal. IAHS Publ. 312, 237–243.
Chang, S.W., Clement, T.P., 2012. Experimental and numerical investigation of saltwater intrusion dynamics in flux-controlled groundwater systems. Water Resour. Res. 48, W09527.
Emara, S.R., Armanuos, A.M., Zeidan, B.A., Gado, T.A., 2024. Numerical investigation of mixed physical barriers for saltwater removal in coastal heterogeneous aquifers. Environ. Sci. Pollut. Res. 31, 4826–4847. https://doi.org/10.1007/s11356-023-31454-z.
Ferguson, G., Gleeson, T., 2012. Vulnerability of coastal aquifers to groundwater use and climate change. Nat. Clim. Chang. 2, 342–345.
Gao, M., Zheng, T., Chang, Q., Zheng, X., Walther, M., 2021. Effects of mixed physical barrier on residual saltwater removal and groundwater discharge in coastal aquifers. Hydrol. Process 35 (7). https://doi.org/10.1002/hyp.14263. Article e14263.
Goswami, R.R., Clement, T.P., 2007. Laboratory-scale investigation of saltwater intrusion dynamics. Water Resour. Res. 43, W04418.
Guo, W., Langevin, C.D., 2002, User's guide to SEAWAT; a computer program for simulation of three-dimensional variable-density ground-water flow.
Janardhana Raju, N., Reddy, T.V.K., Muniratnam, P., Gossel, W., Wycisk, P., 2013. Managed aquifer recharge (MAR) by the construction of subsurface dams in the semi-arid regions: A case study of the Kalangi river basin, Andhra Pradesh. J Geol Soc India 82, 657–665. https://doi.org/10.1007/s12594-013-0204-6.
Kaleris, V.K., Ziogas, A.I., 2013. The effect of cutoff walls on saltwater intrusion and groundwater extraction in coastal aquifers. J. Hydrol. 476, 370–383. https://doi.org/10.1016/j.jhydrol.2012.11.007.
Ketabchi, H., Ataie-Ashtiani, B., 2015. Coastal groundwater optimization-advances, challenges, and practical solutions. Hydrgeol. J. 23 (6), 1129–1154.
Kim, K.Y., Seong, H., Kim, T., Park, K.H., Woo, N.C., Park, Y.S., Koh, G., Park, W., 2006. Tidal effects on variations of fresh–saltwater interface and groundwater flow in a multilayered coastal aquifer on a volcanic island (Jeju Island, Korea). J. Hydrol. 330 (3–4), 525–542. https://doi.org/10.1016/j.jhydrol.2006.04.022.
Langevin, C.D., Shoemaker, W.B., W.B., Guo, W., 2003, MODFLOW-2000, the US Geological Survey Modular Ground-Water Model–Documentation of the SEAWAT-2000 Version with the Variable-Density Flow Process (VDF) and the Integrated MT3DMS Transport Process (IMT). USGS Open-File Report 03-426. Tallahassee, Florida.
Lu, C., Shi, W., Xin, P., Wu, J., Werner, A.D., 2017. Replenishing an unconfined coastal aquifer to control seawater intrusion: injection or infiltration? Water Resour. Res. 53 (6), 4775–4786.

Luyun Jr., R., Momii, K., Nakagawa, K., 2009. Laboratory-scale saltwater behavior due to subsurface cutoff wall. J. Hydrol. 377, 227–236.
Luyun, R., Momii, K., Nakagawa, K., 2011. Effects of recharge wells and flow barriers on seawater intrusion. Ground Water 49, 239–249.
Mantoglou, A., Papantoniou, M., 2008. Optimal design of pumping networks in coastal aquifers using sharp interface models. J. Hydrol. 361, 52–63.
Mehdizadeh, S.S., Werner, A.D., Vafaie, F., Badaruddin, S., 2014. Vertical leakage in sharpinterface seawater intrusion models of layered coastal aquifers. J. Hydrol. 519, 1097–1107.
Mehdizadeh, S.S., Karamalipour, S.E., Asoodeh, R., 2017. Sea level rise effect on seawater intrusion into layered coastal aquifers (simulation using dispersive and sharp-interface approaches). Ocean Coast. Manag. 138, 11–18.
Oostrom, M., Hayworth, J.S., Dane, J.H., Güven, O., 1992. Behaviour of dense aqueous phase leachate plumes in homogeneous porous media. Water Resour. Res. 28, 2123–2134.
Pool, M., Carrera, J., 2010. Dynamics of negative hydraulic barriers to prevent seawater intrusion. Hydrogeol. J. 18, 95–105.
Ratner-Narovlansky, Y., Weinstein, Y., Yechieli, Y., 2020. Tidal fluctuations in a multi-unit coastal aquifer. J. Hydrol. 580, 124222 https://doi.org/10.1016/j.jhydrol.2019.124222.
Riva, M., Guadagnini, A., Dell'Oca, A., 2015. Probabilistic assessment of seawater intrusion under multiple sources of uncertainty. Adv. Water Resour. 75, 93–104.
Robinson, G., Hamill, G.A., Ahmed, A.A., 2015. Automated image analysis for experimental investigations of saltwater intrusion in coastal aquifers. J. Hydrol. 530, 350–360.
Simmons, C.T., Fenstemaker, T.R., Sharp, J.M., 2001. Variable-density groundwater flow and solute transport in heterogeneous porous media: approaches, resolutions and future challenges. J. Contam. Hydrol. 52 (1–4), 245–275. https://doi.org/10.1016/S0169-7722(01)00160-7.
Stevanović, Z., 2016. Damming underground flow to enhance recharge of karst aquifers in the arid and semi-arid worlds. Environ Earth Sci 75, 35. https://doi.org/10.1007/s12665-015-5086-z.
Strack, O.D.L., Ausk, B.K., 2015. A formulation for vertically integrated groundwater flow in a stratified coastal aquifer. Water Resour. Res. 51, 6756–6775.
Voss, C.I., Souza, W.R., 1987. Variable density flow and solute transport simulation of regional aquifers containing a narrow freshwater-saltwater transition zone. Water Resour. Res. 23, 1851–1866.
Wang, J., Kong, J., Gao, Z.L., 2023. Effect of mixed physical barrier on seawater intrusion and nitrate accumulation in coastal unconfined aquifers. Environ. Sci. Pollut. Res. 30, 105308–105328. https://doi.org/10.1007/s11356-023-29637-9.
Werner, A.D., Bakker, M., Post, V.E.A., Vandenbohede, A., Lu, C., Ataie-Ashtiani, B., Simmons, C.T., Barry, D.A., 2013. Seawater intrusion processes, investigation and management: Recent advances and future challenges. Adv. Water Resour. 51, 326.
Yu, X., Xin, P., Lu, C., 2019. Seawater intrusion and retreat in tidally-affected unconfined aquifers: laboratory experiments and numerical simulations. Adv. Water Resour. 132, 103393 https://doi.org/10.1016/j.advwatres.2019.103393.
Zheng, C., Wang, P.P., 1999. MT3DMS: A Modular Three- Dimensional Multispecies Transport Model for Simulation of Advection, Dispersion and Chemical Reactions of Contaminants in Groundwater Systems. Waterways Experiment Station, U.S. Army Corps of Engineers, Vicksburg, Mississippi.